

Robust optimisation applied to the reconfiguration of distribution systems with reliability constraints

ISSN 1751-8687
Received on 9th December 2014
Revised on 25th September 2015
Accepted on 22nd October 2015
doi: 10.1049/iet-gtd.2015.0558
www.ietdl.org

Juan Camilo López¹, Marina Lavorato², John F. Franco³, Marcos J. Rider¹ ✉

¹Department of Systems and Energy, School of Electrical and Computer Engineering, UNICAMP – University of Campinas, Campinas, São Paulo, Brazil

²School of Applied Science, UNICAMP – University of Campinas, Limeira, São Paulo, Brazil

³Departamento de Engenharia Elétrica, Faculdade de Engenharia de Ilha Solteira, UNESP – Universidade Estadual Paulista, Ilha Solteira, São Paulo, Brazil

✉ E-mail: mjrider@dsee.fee.unicamp.br

Abstract: This study presents a mixed-integer second-order conic programming (MISOCP) model for the robust reconfiguration of electrical distribution systems, considering the minimisation of active power losses and reliability constraints. The uncertainty at the reliability data is considered by using a linear and adjustable robust approach. The indices used to evaluate the reliability of the system are the system average interruption frequency index (SAIFI) and the system average interruption duration index (SAIDI), both of which are calculated as functions of the switch status (open or closed). Under radiality constraints, the solution generated by the proposed model is robust in terms of the reliability, i.e. the SADI and SAIFI limits imposed by regulators are not violated even if the uncertain data changes stochastically. The use of an MISOCP model guarantees convergence to optimality by using existing convex optimisation solvers. To evaluate the robustness of each solution generated by the proposed model, a set of Monte Carlo simulations were deployed. Finally, all tests were executed in a 136-node real distribution system.

Nomenclature

Sets

Ω_b	set of nodes
Ω_l	set of branches
Ω_{sw}	set of switches
Ω_z	set of load zones
Ω_z^S	set of source zones

Parameters

c^{lss}	cost of active power losses [\$/kW]
$f_{z,k}^D$	artificial flow demanded at $z \in \Omega_z$ for each $k \in \Omega_b$. Where $f_{z,k}^D = 1$ if $\hat{z}_k = z$, otherwise $f_{z,k}^D = 0$
\bar{I}_{ij}	maximum current at branch $ij \in \Omega_l$ [A]
\bar{I}_{ij}^{sw}	maximum current at switch $ij \in \Omega_{sw}$ [A]
$I_{fused,ij}$	Boolean parameter that indicates whether branch $ij \in \Omega_l$ is fuse protected ($I_{fused,ij} = 1$) or not ($I_{fused,ij} = 0$)
N_i	number of clients connected at node $i \in \Omega_b$
P_i^D	active power demanded at node $i \in \Omega_b$ [kW]
Q_i^D	reactive power demanded at node $i \in \Omega_b$ [kVAr]
r_{sw}	automatic restoration time due to the coordinated operation between switching devices and the main breaker [h]
r_{ij}	restoration time of branch $ij \in \Omega_l$ [h]
r_z	average restoration time of zone $z \in \Omega_z$ [h]
R_{ij}	resistance of branch $ij \in \Omega_l$ [mΩ]
\overline{SAIDI}	maximum SAIDI allowed [h/cust/year]
\overline{SAIFI}	maximum SAIFI allowed [fault/cust/year]
\bar{V}	maximum voltage magnitude [kV]
\underline{V}	minimum voltage magnitude [kV]
X_{ij}	reactance of branch $ij \in \Omega_l$ [mΩ]

\hat{z}_i	zone of node $i \in \Omega_b$
\hat{z}_{ij}	zone of branch $ij \in \Omega_l$
Z_{ij}	impedance of branch $ij \in \Omega_l$, where $Z_{ij} = \sqrt{R_{ij}^2 + X_{ij}^2}$ [mΩ]
Γ	parameter used to adjust the robustness of the proposed model
λ_{ij}	average failure rate of branch $ij \in \Omega_l$ [int/year]
$\lambda_{fused,k}$	average failure rate in the case of lateral fuse protection for each node $k \in \Omega_b$ [int/year]
λ_z	average failure rate of zone $z \in \Omega_z$ [int/year]
σ_z	standard deviation of the failure rate at zone $z \in \Omega_z$ [int/year]

Continuous variables

$f_{ij,k}$	artificial flow through switch $ij \in \Omega_{sw}$, calculated for each node $k \in \Omega_b$
$f_{ij,k}^+, f_{ij,k}^-$	variables used by the linear equivalent of $ f_{ij,k} $
$f_{z,k}^S$	artificial flow generated at $z \in \Omega_z^S$, calculated for each node $k \in \Omega_b$
I_{ij}	current magnitude through branch $ij \in \Omega_l$ [A]
I_{ij}^{sqr}	square of I_{ij} [A ²]
I_{ij}^{sw}	current magnitude through switch $ij \in \Omega_{sw}$ [A]
$I_{ij}^{sw,sqr}$	square of I_{ij}^{sw} [A ²]
$P_{z,k}^{(\lambda),\omega}$	dual variable of the SAIFI constraint (48), related to the binary decision variable $\omega_{z,k}$, used in the robust formulation
$P_{z,k}^{(U),z_{act}}$	dual variable of the SAIDI constraint (49), related to the binary decision variable $z_{act,z,k}$, used in the robust formulation
$P_{z,k}^{(U),\omega}$	dual variable of the SAIDI constraint (49), related to the binary decision variable $\omega_{z,k}$, used in the robust formulation
P_i^S	active power generated at node $i \in \Omega_b$ [kW]

P_{ij}	active power flow through branch $ij \in \Omega_l$ [kW]
P_{ij}^{sw}	active power flow through switch $ij \in \Omega_{sw}$ [kW]
Q_i^S	reactive power generated at node $i \in \Omega_b$ [kVAr]
Q_{ij}	reactive power flow through branch $ij \in \Omega_l$ [kVAr]
Q_{ij}^{sw}	reactive power flow through branch $ij \in \Omega_{sw}$ [kVAr]
SAIDI	average SAIDI of the system [h/cust/year]
SAIFI	average SAIFI of the system [fault/cust/year]
U_k	average annual duration of interruptions at $k \in \Omega_b$ [h/year]
V_i	voltage magnitude at node $i \in \Omega_b$ [kV]
V_i^{sqr}	square of V_i [kV ²]
$z^{(\lambda)}$	dual variable of the SAIFI constraint (48), used in the robust formulation
$z^{(U)}$	dual variable of the SAIDI constraint (49), used in the robust formulation
Λ_k	average annual failure rate at $k \in \Omega_b$ [int/year]

Binary variables

y_{ij}	switch $ij \in \Omega_{sw}$ status, where $y_{ij} = 1$ if switch ij is closed or $y_{ij} = 0$ otherwise
$z_{act,z,k}$	binary reliability variable that identifies if zone $z \in \Omega_z$ is part of the <i>upstream</i> path between each node $k \in \Omega_b$ and its corresponding source, where $z_{act,z,k} = 1$ if zone z is part of the <i>upstream</i> path; otherwise $z_{act,z,k} = 0$
$\omega_{z,k}$	binary reliability variable that identifies if zone $z \in \Omega_z$ is at the same feeder as the node $k \in \Omega_b$, where $\omega_{z,k} = 1$ if the zone z belongs to the same feeder of k ; otherwise $\omega_{z,k} = 0$

1 Introduction

Electrical distribution systems (EDSs) are designed to operate economically and reliably. In this context, switching devices allocated in the feeders can be supervised and controlled in order to reduce the operational costs of the EDS and to guarantee a reliable operation. Moreover, switch operations can be used to reduce the average active power losses, to balance the load flow through feeders, or to improve the voltage profile, by modifying the topology that the system will have along a wide operational horizon, e.g. a season or a year. However, the main reasons why distribution utilities invest in switching and protection devices are to prevent permanent service interruptions and to effectively reduce the number of customers affected by faults.

Reliability measures the capacity of the network to maintain continuous operation over a defined period of time. As such, the ideal investment and operation of switching devices should optimally improve the reliability indices. Two of the most common indices used by utilities around the world are the system average interruption frequency index (SAIFI) and the system average interruption duration index (SAIDI) [1, 2]. There are other reliability indices, such as the average energy not supplied (AENS) and the average service availability index (ASAI). However, SAIDI and SAIFI are customer-oriented indices used by many distribution regulators to measure the continuity of the electrical service and to establish reliability limits and penalties, in case of low-quality service.

Reliability indices are calculated as functions of the failure rates and the restoration times of the system components. The frequency and duration of the interruptions experienced by users can be directly related to the system's topology [3]. Eventually, reconfiguration can be used as a new strategy to maintain reliability indices below the continuity limits imposed by regulators. Thus, in addition to the classical aim of reconfiguring the EDS to minimise operational costs, it is possible to reconfigure the network in order to guarantee a reliable operation.

1.1 Literature review

The optimal reconfiguration problem in EDS has been extensively studied since the pioneer work of Merlin and Back [4] in 1975. A

comprehensive survey on EDS reconfiguration techniques considering loss minimisation, load balancing, voltage profile improvement and service restoration can be found in [5]. However, in the last few years, the optimal reconfiguration of EDS considering reliability constraints and data uncertainty has emerged as a new EDS operating problem.

Most optimisation techniques found in the literature are based on multi-objective metaheuristic algorithms, due to the non-linear and combinatorial nature of the problem and the conflict between the objective functions. Hsiao [6] proposed a multi-objective evolution algorithm enhanced with a fuzzy technique in order to establish the system's configuration that minimises the active power losses, while improving the voltage profile, the service reliability and the number of switch operations. The reliability in [6] was determined as the capacity of the system to support unexpected loads, without considering the failure and restoration rates. Mendoza *et al.* [7] used a micro-genetic multi-objective algorithm for solving the problem, considering power losses minimisation and various reliability indices, such as SAIDI, SAIFI, AENS and the customer average interruption duration index. Bernardon *et al.* [8] proposed an heuristic methodology enhanced with a multi-criteria fuzzy algorithm for minimising the SAIFI and the total active power losses of the system, including the distribution and subtransmission losses. Amanulla *et al.* [9] applied a binary particle-swarm optimisation to solve the problem and used a minimal *cut set* algorithm to determine each node's availability index. Vitorino *et al.* [10] proposed an improved genetic algorithm and calculated the AENS of each configuration using non-sequential Monte Carlo simulations, based on the probability distribution of the random variables. Kavousi-Fard and Akbari-Zadeh [11] used a shuffle frog leaping algorithm enhanced with a multi-criteria fuzzy technique. The authors in [12] proposed a bat algorithm considering DG and a probabilistic load flow and, the same authors in [13] proposed a clonal selection algorithm with a probabilistic load flow and a sensitivity analysis. The failure rates in [11–13] are dependent on the current magnitudes in each line, thus, the reliability indices SAIDI, SAIFI and AENS are modified by the system's operating point.

The methodology in [14] uses a binary gravital search algorithm and calculates the energy not supplied cost, using a Weibull probability distribution to represent the random behaviour of the failure rates. Alonso *et al.* [15] presented an artificial immune system algorithm. The reliability in [15] is calculated with a specialised index called: power interruption equivalent frequency index, that uses a binary matrix to represent the out-of-service nodes in case of a given fault. Gupta *et al.* [16] proposed a genetic algorithm with weighing factors in the objective function to determine the dominance between the active power losses and the reliability indices. Narimani *et al.* [17] proposed an enhanced gravitational search algorithm in order to minimise the active power losses, the operational costs and to improve the system's AENS. The methodology used to calculate each node's reliability in [17] is based on the difference between the duration of the interruptions in the nodes *upstream* the fault and the rest of the nodes, as established by the analytical reliability assessment in [18]. Duan *et al.* [19] applied an enhanced genetic algorithm and reliability indices SAIDI, SAIFI, ASAI and AENS were used. The authors in [19] considered three ways that faults affect each node's reliability: first, if the fault is in another feeder; second, if the fault is in the upstream path of the node; and third, if the fault is not in the upstream path of the node.

None of the aforementioned heuristic and metaheuristic algorithms guarantee optimality of the final solution. Moreover, metaheuristic techniques are neither flexible nor easy to reproduce and modify, since most of them are based on random parameters that require trial-and-error settings, depending on the characteristics of each problem. On the other hand, mathematical models are flexible, easy to represent using mathematical programming languages, and convergence to optimality is guaranteed if the mathematical model is convex.

1.2 Contributions

This paper presents a convex mixed-integer second-order conic programming (MISOCP) model for the robust reconfiguration of EDS with reliability constraints, considering uncertainty of the reliability parameters. The proposed model is used to find a system topology, i.e. the status of the switches allocated along the feeders, in order to minimise the active power losses, while avoiding the violation of the reliability indices (SAIDI and SAIFI) limits. Besides the electrical parameters, the proposed model uses the failure and restoration rates of the EDS circuits in order to analytically compute the reliability of the system. The use of the MISOCP model guarantees optimality by using classical optimisation tools.

To consider uncertainty in the reliability assessment, the model is transformed into a robust MISOCP problem. Robust models guarantee that solutions remain reliable, even if some or all, random parameters exceed the standard deviation around the mean value in accordance with the desired level of robustness. The robust approach used in this paper is based on the linear and adjustable approach presented by Bertsimas and Sim in [20]. To evaluate the level of robustness of each solution, a set of Monte Carlo simulations were conducted. The proposed model was implemented using the mathematical programming language AMPL [21], and solutions were found via the commercial optimisation solver CPLEX [22].

The main contributions of this paper are as follows:

- (i) An MISOCP model for solving the reconfiguration problem of EDS with reliability indices constraints, which has the following benefits: (a) a flexible, realistic and precise model; (b) efficient computational behaviour with conventional MISOCP solvers; and (c) a convergence to optimality guaranteed by using classical optimisation techniques;
- (ii) A robust programming approach that considers uncertainty of the failure rate parameters, used to evaluate the reliability indices of the EDS.

2 Problem overview

In this section, the general formulation of the problem will be introduced. This section also provides the characteristics of the uncertain reliability parameters used throughout this paper, i.e. the probability distribution function used to represent the uncertainty of the annual failure rates for each component.

2.1 Formulation

The robust reconfiguration of the EDS considering reliability constraints is an operational planning problem that defines the status of the switches allocated throughout the system, in order to minimise the average active power losses, and to probabilistically avoid the violation of the reliability limits imposed by regulators. Meanwhile, all technical and operational constraints, such as voltage and current magnitude limits, substation capacities and radial operation, need to be maintained. Radiality is an operational constraint that utilities impose for technical reasons, such as simplifying protection coordination and voltage regulation, and reducing short-circuit currents.

Considering the previous comments, the objective function and the constraints of the problem are defined as follows

$$\min_{y_{ij} \in \Omega_{sw}} c^{lss} \sum_{ij \in \Omega_l} R_{ij}^{sqf} \quad (1)$$

subject to:

$$\text{Reconfiguration of the EDS: (7)–(19)} \quad (2)$$

$$\text{Reliability assessment: (22), (23) and (27)–(38)} \quad (3)$$

$$\text{Robust reliability constraints: (50)–(56)} \quad (4)$$

The objective function in (1) minimises the active power losses multiplied by the cost of the active power losses (c^{lss}). The set of equations in (2) determines the switch status and the AC steady-state operating point of the EDS, while guaranteeing a radial and electrically constrained operation. The assumptions and equations used to reconfigure the EDS are detailed in Section 3. The set of equations in (3) determines the SAIDI and SAIFI indices based on the switch statuses and reliability data. The hypotheses and equations used to analytically evaluate the reliability indices are shown in Section 4. Finally, the robust constraints in (4) consider the uncertainty of the reliability data and provide a reliable topology, even if the failure rates of the circuits change stochastically. The formulation of the robust constraints is detailed in Section 5.

Note that the mathematical model presented in (1)–(4) is a mixed integer non-linear programming problem (MINLP), since the variables used to represent the switch statuses (y_{ij}) are binary and the equations used to provide the AC steady-state operating point of the EDS in (2) are non-linear expressions. Thus, in order to solve the problem using a convex optimisation solver, such as CPLEX, the current MINLP model will be transformed into an MISOCP model, as explained in Section 3.1.

2.2 Uncertainty characterisation

In this paper, the failure rates of the system components are considered uncertain parameters. As shown in [3], the annual failure rates can be stochastically modelled using a Poisson probability distribution function. Then, the probability of k failures in a zone z is given by (5), and the standard deviation (σ_z) for every stochastic parameter λ_z is given by (6)

$$P_z(k) = \frac{\lambda_z^k e^{-\lambda_z}}{k!} \quad \forall z \in \Omega_z \quad (5)$$

$$\sigma_z = \sqrt{\lambda_z} \quad \forall z \in \Omega_z \quad (6)$$

In order to model the problem as a robust programming problem we need to define an interval of protection for every stochastic parameter λ_z . The selected interval should embrace an acceptable area of the Poisson distribution function. Since λ_z cannot be negative, the chosen interval of protection for every stochastic parameter λ_z is defined as $[\max\{0, \lambda_z - \sigma_z\}, \lambda_z + \sigma_z]$.

Fig. 1 shows the proposed interval of protection for $\lambda_z = 0.25, 0.5, 0.75$ and 1.0 failures/year, which are typical failure rates in practical EDS operation.

3 Reconfiguration of the EDSs

This section provides the mathematical foundation used for calculating the EDS steady-state operating point, considering the operation of switching devices. As shown in Fig. 2, the mathematical expressions are based on the circuit equations commonly used by the backward/forward sweep AC load flow algorithms [23, 24] and developed according to the following hypotheses:

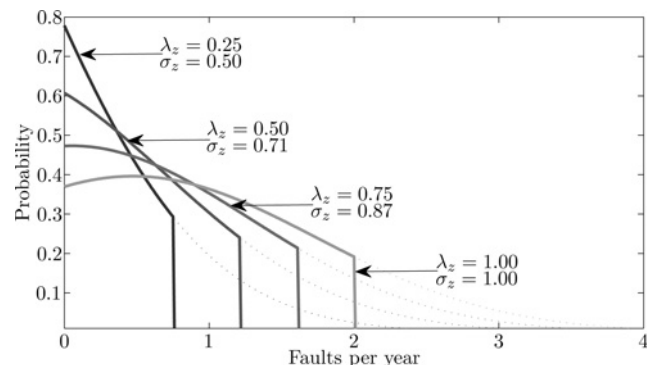


Fig. 1 Poisson distribution function for $\lambda_z = 0.25, 0.5, 0.75$ and 1.0 int/year

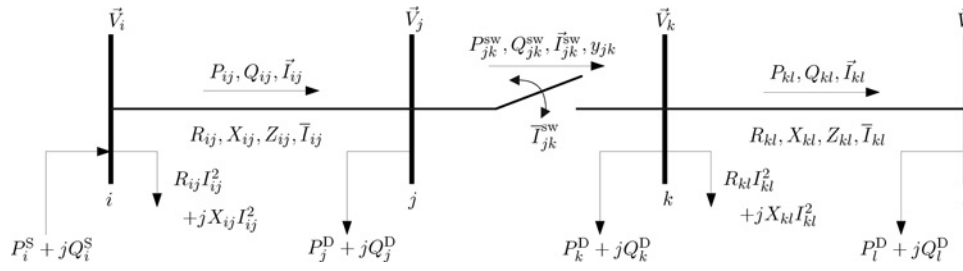


Fig. 2 EDS steady-state analysis with switching devices

- (i) Electrical loads in the EDS are represented as constant active (P_i^D) and reactive (Q_i^D) power loads at every node $i \in \Omega_b$.
- (ii) The system is assumed to be balanced and represented by its single-phase equivalent circuit. Thus, each circuit $ij \in \Omega_l$ has a resistance R_{ij} , a reactance X_{ij} and a current capacity \bar{I}_{ij} associated to it.
- (iii) All switches $ij \in \Omega_{sw}$ are considered short-length circuits with negligible impedance and limited current capacity.

The steady-state operation of EDS considering switching devices is defined by the calculation of the active (P_i^S) and reactive (Q_i^S) power generated at each source node, the voltage magnitudes at each node, the active (P_{ij}, P_{ij}^{sw}) and reactive (Q_{ij}, Q_{ij}^{sw}) power flows through each circuit and switch, and the status (y_{ij}) of each switch installed in the system, in terms of the branch and node parameters. Active and reactive power losses at each circuit ij , given by the expression $R_{ij}I_{ij}^2 + jX_{ij}I_{ij}^2$, are associated to the node i in order to guarantee power balance throughout the system.

Since the current and voltage magnitudes are always presented as squared variables, hence, the following change in variables is convenient without loss of generality: $V_i^{sqr} = V_i^2, \forall i \in \Omega_b$; $I_{ij}^{sqr} = I_{ij}^2, \forall ij \in \Omega_l$; and $I_{ij}^{sqr,sw} = (I_{ij}^{sw})^2, \forall ij \in \Omega_{sw}$. Where V_i^{sqr}, I_{ij}^{sqr} and $I_{ij}^{sqr,sw}$ are continuous non-negative variables.

The sets of equations in (7) and (8) determine the voltage and the current magnitudes in the circuits as functions of the active and reactive power flows, and the system parameters

$$V_i^{sqr} - V_j^{sqr} = 2(R_{ij}P_{ij} + X_{ij}Q_{ij}) + Z_{ij}^2 I_{ij}^{sqr} \quad \forall ij \in \Omega_l \quad (7)$$

$$V_j^{sqr} I_{ij}^{sqr} = P_{ij}^2 + Q_{ij}^2 \quad \forall ij \in \Omega_l \quad (8)$$

Similarly, constraints (9) and (10) calculate the voltage and current magnitudes of the switch's nodes. Note that, since the impedances of the switches are neglected, if the switch ij is closed ($y_{ij}=1$), then both nodal voltage magnitudes will be equal; otherwise, if switch ij is open ($y_{ij}=0$), then the difference between both nodal voltages can vary freely within their operational limits

$$|V_i^{sqr} - V_j^{sqr}| \leq (\bar{V}^2 - \underline{V}^2)(1 - y_{ij}) \quad \forall ij \in \Omega_{sw} \quad (9)$$

$$V_j^{sqr} I_{ij}^{sw,sqr} = (P_{ij}^{sw})^2 + (Q_{ij}^{sw})^2 \quad \forall ij \in \Omega_{sw} \quad (10)$$

To guarantee connectivity along the feeders, (11) and (12) are used to represent the active and reactive power flow balances in the nodes, considering the power losses and the power flows of the closed switches

$$\sum_{ji \in \Omega_l} P_{ji} - \sum_{ij \in \Omega_l} (P_{ij} + R_{ij} I_{ij}^{sqr}) + \sum_{ji \in \Omega_{sw}} P_{ji}^{sw} - \sum_{ij \in \Omega_{sw}} P_{ij}^{sw} + P_i^S = P_i^D \quad \forall i \in \Omega_b \quad (11)$$

$$\sum_{ji \in \Omega_l} Q_{ji} - \sum_{ij \in \Omega_l} (Q_{ij} + X_{ij} I_{ij}^{sqr}) + \sum_{ji \in \Omega_{sw}} Q_{ji}^{sw} - \sum_{ij \in \Omega_{sw}} Q_{ij}^{sw} + Q_i^S = Q_i^D \quad \forall i \in \Omega_b \quad (12)$$

Constraints (13) and (14) represent the current and voltage magnitudes limits at every branch and node in the system

$$0 \leq I_{ij}^{sqr} \leq \bar{I}_{ij}^2 \quad \forall ij \in \Omega_l \quad (13)$$

$$\underline{V}^2 \leq V_i^{sqr} \leq \bar{V}^2 \quad \forall i \in \Omega_b \quad (14)$$

Constraints (15), (16) and (17) define the operational limits for the active and reactive power and current magnitudes of the switches if they are closed ($y_{ij}=1$); if switch ij is open, however, these three magnitudes are zero

$$|P_{ij}^{sw}| \leq (\bar{V} I_{ij}^{sw}) y_{ij} \quad \forall ij \in \Omega_{sw} \quad (15)$$

$$|Q_{ij}^{sw}| \leq (\bar{V} I_{ij}^{sw}) y_{ij} \quad \forall ij \in \Omega_{sw} \quad (16)$$

$$0 \leq I_{ij}^{sw,sqr} \leq (\bar{I}_{ij}^{sw})^2 y_{ij} \quad \forall ij \in \Omega_{sw} \quad (17)$$

Constraint (18) is the analytical expression that, together with (11) and (12), guarantees the radial topology of the final solution, as demonstrated by Lavorato *et al.* [25]. The operator of cardinality $|\Omega|$ in (18) determines the number of elements of the set Ω

$$|\Omega_l| + \sum_{ij \in \Omega_{sw}} y_{ij} = |\Omega_b| - |\Omega_b^S| \quad (18)$$

As discussed in [26], in order to avoid loop generation due to the presence of transfer nodes in the EDS, i.e. interconnection nodes with no demand, a small load of 0.001 kW is assumed in each transfer node so that all nodes are truly connected by (11). If, for any reason, a small load cannot be used, then an alternative mathematical approach for generating radial topologies considering interconnection nodes can be found in [27]. Finally, the binary nature of the decision variable y_{ij} is established by the following equation

$$y_{ij} \in \{0, 1\} \quad \forall ij \in \Omega_{sw} \quad (19)$$

3.1 MISOCP model transformation for the optimal reconfiguration of EDS

Together, the objective function in (1) and the mathematical expression in (7)–(19) produce a MINLP problem for the optimal reconfiguration of EDS [25, 28]. However, MINLP models are not convex and modern optimisation tools cannot guarantee the optimal solution for this kind of formulation.

To achieve convexity and optimality, the equality constraints in (8) and (10) are transformed into the second-order conic

constraints shown in the following equations

$$V_j^{\text{sqf}} I_{ij}^{\text{sqf}} \geq P_{ij}^2 + Q_{ij}^2 \quad \forall ij \in \Omega_l \quad (20)$$

$$V_j^{\text{sqf}} I_{ij}^{\text{sw,sqf}} \geq \left(P_{ij}^{\text{sw}}\right)^2 + \left(Q_{ij}^{\text{sw}}\right)^2 \quad \forall ij \in \Omega_{\text{sw}} \quad (21)$$

The new MISOCP model, defined by (1), (7), (9) and (11)–(21), is a convex programming problem and, thus, can be optimally solved via branch and bound techniques implemented by classical optimisation tools.

If the new MISOCP model has a feasible solution, and the dual variables related to constraints (20) and (21) are greater than zero, then the solution provided by the MISOCP model is the optimal solution of the original MINLP model, as demonstrated by Franco *et al.* [29] for the EDS expansion planning problem.

4 Reliability assessment

This section presents the formulation used to calculate the reliability indices, SAIDI and SAIFI, and the hypotheses made for computing the reliability in terms of the system's topology.

To relate the reliability assessment to the binary decision variable y_{ij} , is necessary to add a new set of constraints to the reconfiguration model presented in the previous section. The procedure used to define the reliability indices of EDS in this paper is based on the fundamental analysis for radial networks considering switching devices and fuses, described by Billinton and Allan [3]. The reliability of EDS is defined by the following indices

$$\text{SAIFI} = \frac{\sum_{k \in \Omega_b} \Lambda_k N_k}{\sum_{k \in \Omega_b} N_k} \quad (22)$$

$$\text{SAIDI} = \frac{\sum_{k \in \Omega_b} U_k N_k}{\sum_{k \in \Omega_b} N_k} \quad (23)$$

The SAIFI in (22) indicates how often average users suffer from a sustained interruption in a year, and is based on the annual failure rate (Λ_k) of every node $k \in \Omega_b$. SAIDI in (23) indicates the average duration of the interruptions experienced by users in a year, and is based on the annual duration of the interruptions (U_k) of every node $k \in \Omega_b$. Normally Λ_k and U_k are determined by the statistical or predictive value of the annual failure rate and restoration time of the EDS components. However, protection devices, such as fuses, reclosers and sectionalisers installed along feeders, complicate the reliability assessment. Thus, this section presents a set of constraints to analytically calculate the SAIFI and SAIDI according to the system's topology, considering the operation of switching devices and fuses in EDS.

4.1 Pre-processing procedure

Before formulating the reliability constraints, the following pre-processing steps need to be carried out:

Step 1: Define the set of zones (Ω_z): Each zone is a section of the EDS, in which the nodes are radially connected and delimited by switching devices. In effect, all of the users that belong to the same zone would experience the same frequency and duration of interruptions in a year. Thus, nodes are aggregated into zones in order to simplify the reliability assessment.

Step 2: Calculate parameters λ_z and r_z for all of the zones: Expressions (24) and (25) calculate the average failure rate (λ_z) and average restoration time (r_z), respectively, for each zone z

defined in Step 1.

$$\lambda_z = \sum_{\substack{ij \in \Omega_{z_l} \\ ij \text{ is not fuse} \\ \text{protected}}} \lambda_{ij} \quad \forall z \in \Omega_z \quad (24)$$

$$r_z = \frac{1}{|\Omega_{z_l}|} \sum_{ij \in \Omega_{z_l}} r_{ij} \quad \forall z \in \Omega_z \quad (25)$$

Set function $\Omega_{z_l} = \{ij \in \Omega_l | \hat{z}_{ij} = z\}$ contains all of the branches that belong to the specific zone z .

$$\lambda_{\text{fused}_k} = \begin{cases} \sum_{ij \in \Omega_l} \lambda_{ij} & \text{If } I_{\text{fused}_{ij}} = 1, \text{ and } k, i \text{ and } j \text{ belong to the same path} \\ 0 & \text{Otherwise} \end{cases} \quad (26)$$

$\forall k \in \Omega_b$

Parameter λ_{fused_k} makes it possible to distinguish fuse-protected nodes in lateral circuits from those that belong to the main feeder in each zone. The conditional summation in (26) considers the *downstream* embracing effect of fuses, which protects circuits from sustained faults *downstream* of the point where the fuse is installed.

4.2 Hypotheses

The following hypotheses form the basis of the proposed reliability assessment:

- (i) Faults are considered sustained short circuits, therefore, every fault in a non-fuse-protected circuit of the EDS will trigger a main breaker operation.
- (ii) Permanent faults in lateral fuse-protected circuits are isolated due to the fuse blow [see (26)].
- (iii) Fuses located in the main feeder of each zone are disregarded from this analysis.
- (iv) Faults in one feeder do not affect the other feeders.
- (v) Switching devices, coordinated with the main breaker operation, produce the quick isolation of the zones that do not belong to the *upstream* path of a node whose reliability is being evaluated. In other words, if a fault occurs in a zone that does not belong to the *upstream* path of the node whose reliability is being evaluated, the restoration scheme will restore the interruption in at least r_{sw} time.

As an example, consider the 16-node radial system shown in Figs. 3a and b. If the node whose reliability is being evaluated is node 10, then the upstream path in Fig. 3a is formed by zones 4 and 1 (shaded areas), and all interruptions due to faults in the rest of the zones, i.e. zones 2, 3 and 5, are quickly restored using the coordinated operation of the switches. Otherwise, if the fault is located in any of the upstream zones, then it would take a nominal restoration time to repair the interruption. Thus, the frequency and duration of the interruptions of node 10 shown in Fig. 3a are

$$\Lambda_{10(a)} = \lambda_{F1} + \lambda_{Z1} + \lambda_{Z3} + \lambda_{Z4}$$

$$U_{10(a)} = \lambda_{F1} r_{F1} + \lambda_{Z1} r_{Z1} + \lambda_{Z4} r_{Z4} + \lambda_{Z3} r_{\text{sw}}$$

Note that, as shown in Fig. 3b, if the topology of the system changes, then the upstream path of node 10 also changes, and the reliability experienced by the users connected to node 10 is different from the one shown in Fig. 3a. The frequency and duration of the

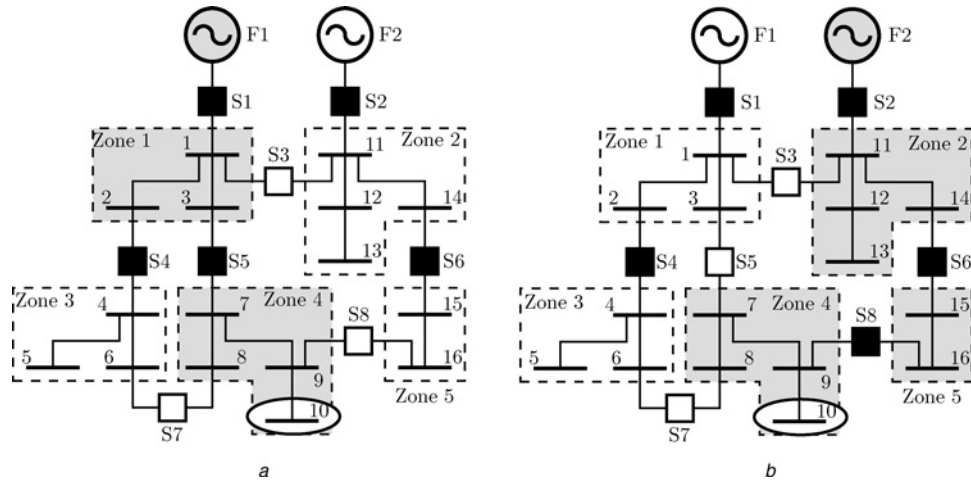


Fig. 3 Hypotheses 5. Influence of the system's topology in the reliability assessment

a Upstream path of the node 10 is formed by zones 1 and 4
b Upstream path of the node 10 is formed by zones 2, 4 and 5

interruptions of node 10 shown in Fig. 3b are

$$\Lambda_{10(b)} = \lambda_{F2} + \lambda_{Z2} + \lambda_{Z4} + \lambda_{Z5}$$

$$U_{10(b)} = \lambda_{F2} r_{F2} + \lambda_{Z2} r_{Z2} + \lambda_{Z4} r_{Z4} + \lambda_{Z5} r_{Z5}$$

4.3 Reliability constraints

The set of constraints (27)–(38) is a mathematical adaptation of the procedure proposed in [3] to analytically estimate the reliability of radial networks, considering switching devices, fuse operation and the hypotheses established in the prior subsection

$$\sum_{\substack{ji \in \Omega_{sw} \\ \hat{z}_i = z}} f_{ji,k} - \sum_{\substack{ij \in \Omega_{sw} \\ \hat{z}_j = z}} f_{ij,k} + f_{z,k}^S = f_{z,k}^D \quad \forall k \in \Omega_b, \forall z \in \Omega_z \quad (27)$$

$$|f_{ij,k}| \leq y_{ij} \quad \forall ij \in \Omega_{sw}, \forall k \in \Omega_b \quad (28)$$

$$z_{act\hat{z}_j,k} \geq |f_{ij,k}| \quad \forall ij \in \Omega_{sw}, \forall k \in \Omega_b \quad (29)$$

$$z_{act\hat{z}_i,k} \geq |f_{ij,k}| \quad \forall ij \in \Omega_{sw}, \forall k \in \Omega_b \quad (30)$$

$$\omega_{\hat{z}_j,k} \geq \omega_{z_i,k} + y_{ij} - 1 \quad \forall ij \in \Omega_{sw}, \forall k \in \Omega_b \quad (31)$$

$$\omega_{\hat{z}_i,k} \geq \omega_{z_j,k} + y_{ij} - 1 \quad \forall ij \in \Omega_{sw}, \forall k \in \Omega_b \quad (32)$$

$$z_{actz,k} \leq \omega_{z,k} \quad \forall k \in \Omega_b, \forall z \in \Omega_z \quad (33)$$

$$\omega_{z,k} \leq f_{z,k}^S \quad \forall k \in \Omega_b, \forall z \in \Omega_z^S \quad (34)$$

$$z_{actz,k} \leq \sum_{\substack{ij \in \Omega_{sw} \\ \hat{z}_i = z}} |f_{ij,k}| + \sum_{\substack{ji \in \Omega_{sw} \\ \hat{z}_j = z}} |f_{ji,k}| \quad \forall k \in \Omega_b, \forall z \in \Omega_z \quad (35)$$

$$\Lambda_k = \sum_{z \in \Omega_z} \omega_{z,k} \lambda_z + \lambda_{fused_k} \quad \forall k \in \Omega_b \quad (36)$$

$$U_k = \sum_{z \in \Omega_z} \left[z_{actz,k} \lambda_z r_z + (\omega_{z,k} - z_{actz,k}) \lambda_z r_{sw} \right] + \lambda_{fused_k} r_{\hat{z}_k} \quad \forall k \in \Omega_b \quad (37)$$

$$z_{actz,k}, \omega_{z,k} \in \{0, 1\} \quad \forall k \in \Omega_b, \forall z \in \Omega_z \quad (38)$$

Since the reliability indices, SAIFI and SAIDI, depend on the

system's topology, (27)–(38) define the annual failure rate of every node (Λ_k), and the annual duration of the interruptions of every node (U_k), according to the value of the binary decision variable y_{ij} .

Constraint (27) represents an artificial flow balance throughout the zones and the switches of the system. The continuous variable $f_{ij,k}$ is an artificial flow that identifies the *upstream* path between each node k and its corresponding source, where $ij \in \Omega_{sw}$. The identification of the *upstream* path is necessary in order to evaluate the average annual outage time (U_k) for each node, as established by the fifth hypotheses in Section 4.2. Since parameter $f_{z,k}^D$ is equal to 1 if $\hat{z}_k = z$, 0 otherwise; constraint (27) is the analytical formulation that finds the shortest path through a radial graph between each node k and its corresponding source [30].

To maintain linearity, the artificial flow is represented by the linear set (39)–(41). The absolute value of $f_{ij,k}$ is replaced by its linear equivalent, $|f_{ij,k}| = f_{ij,k}^+ + f_{ij,k}^-$, in all equations

$$f_{ij,k} = f_{ij,k}^+ - f_{ij,k}^- \quad \forall ij \in \Omega_{sw}, \forall k \in \Omega_b \quad (39)$$

$$f_{ij,k}^+ \geq 0 \quad \forall ij \in \Omega_{sw}, \forall k \in \Omega_b \quad (40)$$

$$f_{ij,k}^- \geq 0 \quad \forall ij \in \Omega_{sw}, \forall k \in \Omega_b \quad (41)$$

Constraint (28) links the artificial flow $f_{ij,k}$ with the binary decision variables y_{ij} . If switch ij is open ($y_{ij} = 0$), then (28) forbids flow through it; otherwise, constraints (27) decides if switch ij is part of the *upstream* path of the node k .

The binary reliability variables $z_{actz,k}$ and $\omega_{z,k}$ are defined by (29), (30) and (31), (32), respectively. $z_{actz,k}$ determines the zones that are part of the *upstream* path between each node k and its corresponding source. If the artificial flow through the switch ij is positive, then (29) and (30) establish that both zones, \hat{z}_i and \hat{z}_j , are part of the *upstream* path of the node k . On the other hand, $\omega_{z,k}$ determines if the zone z and the node k belong to the same feeder, i.e. if both are supplied by the same source. If the switch ij is closed, and whether \hat{z}_i or \hat{z}_j is supplied by the same source than k , then (31) and (32) establish that both zones belong to the same feeder of k .

Constraints (33)–(35) establish the following set of trivial relationships between the binary decision variables $z_{actz,k}$ and $\omega_{z,k}$ and the artificial flow $f_{ij,k}$:

(i) Constraint (33) defines that if the zone z does not belong to the same feeder of a node k , eventually the zone cannot be part of the *upstream* path, thus if $\omega_{z,k} = 0$, then $z_{actz,k} = 0$.

(ii) Constraint (34) establishes that if no artificial flow is generated at substation zone $z \in \Omega_z^S$ for a given node k , it means that k does not belong to the feeder supplied by z , thus if $f_{z,k}^S = 0$, then $\omega_{z,k} = 0$.

(iii) Constraint (35) determines that $z_{actz,k} = 0$, if all artificial flows associated to the zone z are zero, for a given node k .

Constraints (33)–(35) avoid inconsistencies between the binary variables and enhance the accuracy of the final solution produced by the solver.

Equation (36) defines the average annual failure rate (Λ_k) at every node, while (37) defines the average annual duration of interruptions (U_k) at every node. Both variables are functions of the average failure rates ($\lambda_z, \lambda_{fusedk}$), the restoration times (r_z, r_{sw}) and the binary reliability variables $z_{actz,k}$ and $\omega_{z,k}$. The reliability indices are assessed by (22) and (23), where N_k is the number of customers connected to the node k .

Finally, constraints (42) and (43) can be appended to the mathematical model in order to guarantee that the average SAIDI and SAIFI do not violate the limits imposed by regulators

$$SAIFI \leq \overline{SAIFI} \quad (42)$$

$$SAIDI \leq \overline{SAIDI} \quad (43)$$

The set of constraints in (27)–(43) is a mixed-integer linear equation system that can be added to the reconfiguration MISOCP problem in (1), (7), (9) and (11)–(23) in order to determine and limit the reliability of the final solution. The new reconfiguration problem with reliability constraints is a convex programming problem that can be solved with commercial solvers, such as CPLEX. The solution produced by the proposed reconfiguration model obtains the EDS's topology that minimises active power losses and guarantees that the average reliability indices, SAIFI and SAIDI, remain below their limits.

5 Robust reliability constraints

A major disadvantage of the proposed reliability constraints in (27)–(43) is the fact that reliability parameters, such as annual failure rates, are stochastic, uncontrollable and highly uncertain parameters. Thus, in practice, the use of average values of λ_z can lead to unrealistic and unreliable solutions. Accordingly, this section considers the uncertainty characterisation of the reliability parameters λ_z shown in Section 2.2 in order to transform the deterministic reliability constraints (42) and (43) into robust reliability constraints.

5.1 Linear robust optimisation

Robust optimisation allows models to remain feasible even if some or all, random parameters change during the application of the solution produced by the robust model. A linear and adjustable approach for turning deterministic models into robust models was presented by Bertsimas and Sim [20].

Consider the nominal optimisation problem given by the following equation

$$\begin{cases} \min \sum_j c_j x_j \\ \text{s.t.} \\ \sum_j a_{ij} x_j \leq b_i \quad \forall i \\ l_j \leq x_j \leq u_j \quad \forall j \end{cases} \quad (44)$$

where x_j is the set of decision variables, c_j is the set of costs at the objective function and a_{ij} is the set of coefficients at every constraint i . Consider that Ω_{U_i} contains all of the coefficients in the i th constraint that are subject to uncertainty. If every uncertain coefficient $a_{ij}, \forall j \in \Omega_{U_i}$ is modelled as a random variable that takes values within the symmetrically bounded interval $[a_{ij} - \hat{a}_{ij}, a_{ij} + \hat{a}_{ij}]$, then the robust formulation presented in [20]

is given by the following equation

$$\begin{cases} \min \sum_j c_j x_j \\ \text{s.t.} \\ \sum_j a_{ij} x_j + z_i \Gamma_i + \sum_{j \in \Omega_{U_i}} p_{ij} \leq b_i \quad \forall i \\ z_i + p_{ij} \geq \hat{a}_{ij} |x_j| \quad \forall i, \forall j \in \Omega_{U_i} \\ l_j \leq x_j \leq u_j \quad \forall j \\ p_{ij} \geq 0 \quad \forall i, \forall j \in \Omega_{U_i} \\ z_i \geq 0 \quad \forall i \end{cases} \quad (45)$$

The new robust model in (45) remains linear since the term $|x_j|$ is easy to linearise, and a new set of continuous variables z_i and $p_{ij}, \forall i, \forall j \in \Omega_{U_i}$ is added. Parameter Γ_i adjusts the level of robustness of every constraint i in the final solution. If $\Gamma_i = 0$, then constraint i will not be robust, and its coefficients are expected to be deterministic parameters ($\hat{a}_{ij} = 0$). Otherwise, if $\Gamma_i = |\Omega_{U_i}|$, then constraint i will be totally protected, even if all of the random coefficients of i reach their known limits. Although, the last scenario is a tempting protective approach, it would lead to an extremely conservative solution, with the worst objective function possible. The mathematical development used to transform nominal deterministic mathematical models into robust programming problems is detailed in the Appendix.

5.2 Robust SAIDI and SAIFI limits

Let (42) and (43) be the constraints that limit the reliability indices, SAIDI and SAIFI, subject to the uncertainty of parameter λ_z . SAIFI and SAIDI in (42) and (43) are replaced by their equivalent (22) and (23) to obtain the following equations

$$\frac{\sum_{k \in \Omega_b} \Lambda_k N_k}{\sum_{k \in \Omega_b} N_k} \leq \overline{SAIFI} \quad (46)$$

$$\frac{\sum_{k \in \Omega_b} U_k N_k}{\sum_{k \in \Omega_b} N_k} \leq \overline{SAIDI} \quad (47)$$

Λ_k and U_k in (46) and (47) are replaced by their equivalents given by (36) and (37) for each node $k \in \Omega_b$, to obtain the following equations

$$\sum_{k \in \Omega_b} \sum_{z \in \Omega_z} N_k \lambda_z \omega_{z,k} \leq \sum_{k \in \Omega_b} N_k (\overline{SAIFI} - \lambda_{fusedk}) \quad (48)$$

$$\begin{aligned} & \sum_{k \in \Omega_b} \sum_{z \in \Omega_z} [N_k (r_z - r_{sw}) \lambda_z z_{actk,z} + N_k r_{sw} \lambda_z \omega_{z,k}] \\ & \leq \sum_{k \in \Omega_b} N_k (\overline{SAIDI} - \lambda_{fusedk} r_{z_k}^2) \end{aligned} \quad (49)$$

Note that (48) and (49) have the form $\sum_j a_{ij} x_j \leq b_i$. The decision variables are the binary reliability variables $z_{actk,z}$ and $\omega_{z,k}$, and all coefficients are multiplied by the random parameter λ_z . Also, the right-side members of (48) and (49) are constants factors.

As explained in Section 2.2, the protection interval of the random parameter λ_z is bounded by the term $[\lambda_z - \sigma_z, \lambda_z + \sigma_z]$. Thus, the coefficients that multiplied the binary variables $z_{actk,z}$ and $\omega_{z,k}$ in (48) and (49) are bounded by the same protection interval. Applying the linear robust formulation given by (45), then (48) and (49) are transformed into robust constraints given by the following equations

$$\begin{aligned} & \sum_{k \in \Omega_b} \sum_{z \in \Omega_z} N_k \lambda_z \omega_{z,k} + z^{(\lambda)} \Gamma + \sum_{k \in \Omega_b} \sum_{z \in \Omega_z} P_{z,k}^{(\lambda), \omega} \\ & \leq \sum_{k \in \Omega_b} N_k (\overline{SAIFI} - \lambda_{fusedk}) \end{aligned} \quad (50)$$

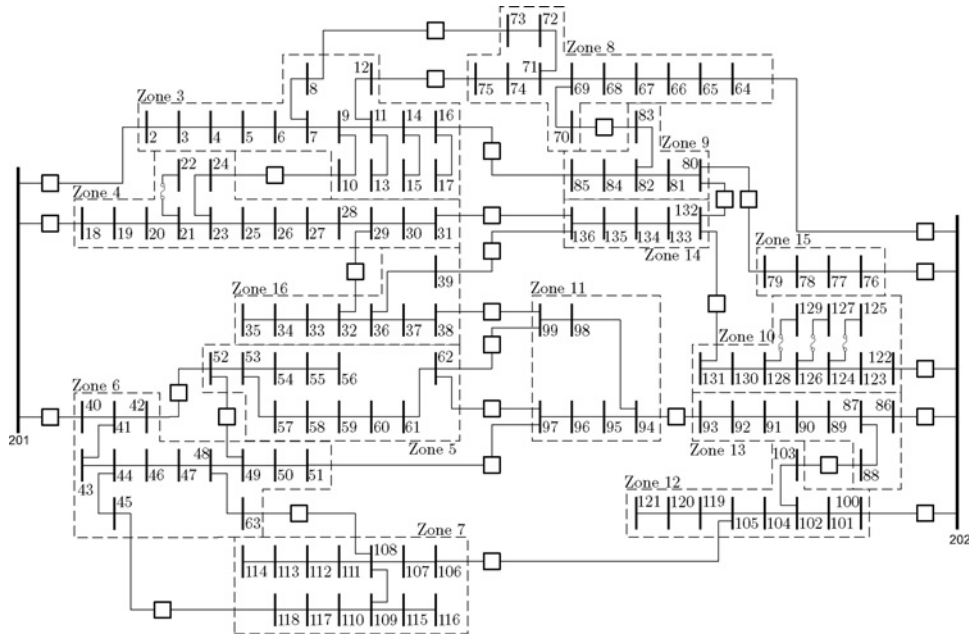


Fig. 4 136-node real system with 16 load zones

$$\sum_{k \in \Omega_b} \sum_{z \in \Omega_z} \left[N_k (r_z - r_{sw}) \lambda_z z_{actk,z} + N_k r_{sw} \lambda_z \omega_{z,k} \right] + 2z^{(U)} \Gamma + \sum_{k \in \Omega_b} \sum_{z \in \Omega_z} \left(p_{z,k}^{(U),z_{act}} + p_{z,k}^{(U),\omega} \right) \leq \sum_{k \in \Omega_b} N_k \left(\overline{\text{SAIDI}}_k - \lambda_{fusedk} r_{z_k} \right) \quad (51)$$

$$z^{(\lambda)} + p_{z,k}^{(\lambda),\omega} \geq N_k \sigma_z \omega_{z,k} \quad \forall k \in \Omega_b, \forall z \in \Omega_z \quad (52)$$

$$z^{(U)} + p_{z,k}^{(U),z_{act}} \geq N_k (r_z - r_{sw}) \sigma_z z_{actk,z} \quad \forall k \in \Omega_b, \forall z \in \Omega_z \quad (53)$$

$$z^{(U)} + p_{z,k}^{(U),\omega} \geq N_k r_{sw} \sigma_z \omega_{z,k} \quad \forall k \in \Omega_b, \forall z \in \Omega_z \quad (54)$$

$$z^{(\lambda)} \geq 0 \quad \text{and} \quad z^{(U)} \geq 0 \quad (55)$$

$$p_{z,k}^{(\lambda),\omega} \geq 0, p_{z,k}^{(U),z_{act}} \geq 0, p_{z,k}^{(U),\omega} \geq 0 \quad \forall k \in \Omega_b, \forall z \in \Omega_z \quad (56)$$

Note that, new dual variables z_i and p_{ij} have been created in (50) and (56) for every binary reliability variables $z_{actk,z}$ and $\omega_{z,k}$. Also, considering that the number of decision variables in (51) is twice than (50), parameter Γ of (51) is multiplied by 2. The use of only one parameter Γ in the robust model is convenient because it makes possible to change the robustness of the model by adjusting only one Γ parameter. Moreover, $0 \leq \Gamma \leq |\Omega_z| |\Omega_b|$. Equations (27)–(38), used to determine the average value of each failure and duration rates, are considered deterministic, so they are not affected by the robust formulation.

6 MISOCPP for the robust reconfiguration of EDS with reliability constraints

Finally, the MISOCPP for the optimal reconfiguration of EDS considering reliability indices assessment and robust reliability constraints is given by the following equation

$$\begin{cases} \min & c^{lss} \sum_{ij \in \Omega_l} R_{ij}^{sqf} \\ \text{s.t.} & (7), (9), (11)–(23), (27)–(41), (50)–(56) \end{cases} \quad (57)$$

7 Tests and results

The 136-node real system shown in Fig. 4 was used to demonstrate the performance of the proposed model. Electrical and reliability data can be obtained in [31]. The constants of the system are $c^{lss} = \$ 1/\text{kWh}$, $V_{nomf-n} = 7.967 \text{ kV}$, $V = 0.9 V_{nom}$, $\bar{V} = 1.1 V_{nom}$, $r_{sw} = 0.5 \text{ h}$, $|\Omega_z| = 18$ and $|\Omega_b| = 138$. Reliability limits were set at $\overline{\text{SAIDI}} = 5.24 \text{ h/cust/yr}$ and $\text{SAIFI} = 4 \text{ int/cust/yr}$, as established by the Brazilian EDS regulator in [32]. The proposed model was implemented in AMPL [21] and solved with CPLEX [22], (with default options and with a maximum gap of 1% as optimality criterion) on a workstation with an Intel Core i5-4570 processor.

The 136-node system in Fig. 4 has two source nodes, corresponding to nodes 201 and 202, and 16 load zones highlighted with dashed lines. Switches in Fig. 4 are indicated with squares, and some lateral branches are protected with fuses. Table 1 contains the average failure rates (λ_z), average restoration times (r_z) and standard deviations (σ_z) of each zone, calculated using (24), (25) and (6), respectively.

To obtain all the feasible robust solutions of (57), parameter Γ is iteratively adjusted as follows:

- (i) Let $k \leftarrow 0$. Set $\Gamma = 0$, and solve (57) robust MISOCPP model.
- (ii) Save SAIDI_k , SAIFI_k and the operating point obtained in the k th iteration.
- (iii) Set $k \leftarrow k + 1$, $\Gamma = k$ and solve (57) robust MISOCPP model. If feasible, return to step ii; otherwise, continue to step 4.
- (iv) Display all feasible robust solutions.

All feasible robust solutions for the 136-node system found using the former procedure are shown in Table 2. All voltage and current

Table 1 λ_z , r_z and σ_z for each zone of the 136-node system shown in Fig. 4

Zone	λ_z , int/year	r_z , h	σ_z , int/year	Zone	λ_z , int/year	r_z , h	σ_z , int/year
3	0.75	2.00	0.87	10	0.30	2.00	0.63
4	0.60	2.00	0.77	11	0.25	2.00	0.50
5	0.50	3.00	0.71	12	0.40	3.00	0.63
6	0.60	2.00	0.77	13	0.35	2.00	0.59
7	0.60	3.00	0.77	14	0.20	2.00	0.45
8	0.55	2.00	0.74	15	0.15	2.00	0.39
9	0.25	2.00	0.50	16	0.35	2.00	0.59

Table 2 Configurations of the feasible robust solutions for the 136-node system

Γ	Topology (open switches)	Power losses, [kW]	SAIDI, [h/cust/yr]	SAIFI, [int/cust/yr]	Robustness, %
[0, 36]	49–52, 105–106, 12–75, 16–85, 31–136, 39–136, 38–99, 62–99, 62–97, 51–97, 45–118, 8–73, 70–83, 88–103, 80–132, 24–10	787.62	2.61	2.97	78.4
[37, 41]	12–75, 16–85, 31–136, 39–136, 38–99, 62–99, 62–97, 45–118, 63–108, 8–73, 70–83, 88–103, 42–52, 80–132, 93–94, 24–10	866.70	2.60	2.91	80.4
[42, 43]	49–52, 105–106, 12–75, 16–85, 31–136, 39–136, 62–99, 62–97, 51–97, 45–118, 8–73, 70–83, 88–103, 80–132, 32–29, 24–10	912.34	2.58	2.92	80.8
[44]	202–64, 16–85, 31–136, 38–99, 62–99, 62–97, 45–118, 63–108, 8–73, 70–83, 88–103, 42–52, 80–132, 93–94, 32–29, 24–10	1233.67	2.67	2.89	81.2

limits are satisfied. The first column in Table 2 identifies the interval of Γ established by the iterative adjustment. As Γ increases, the level of robustness is enhanced. Note that the least robust solution is obtained by setting $0 \leq \Gamma \leq 36$, which corresponds to the configuration that optimally minimises the active power losses in the system (with a value of 787.62 kW). On the other hand, the most robust solution is obtained by setting $\Gamma = 44$, but the active power losses are increased to 1233.67 kW.

Note that, feasibility is lost for $\Gamma > 44$. This means that there is not a feasible solution that prevents (42) and (43) from being violated in all probable values of λ_z . Then, given the average values and the standard deviations of the failure rates in Table 1, 100% reliability robustness is not achievable for this particular system. The fourth and the fifth columns in Table 2 identify the average SAIDI and SAIFI for every robust solution, calculated by (22) and (23). Both indices are shown in order to demonstrate the model's capacity to determine the average reliability indices of the EDS depending on the system's topology.

Since the purpose of the robust formulation is to maintain both reliability indices below their limits, the last column in Table 2 indicates the robustness for each solution. Equation (58) and a set of Monte Carlo simulations were executed to establish the probability of (42) and (43) from being violated if all the parameters λ_z stochastically change during the real application of each robust solution considering the uncertainty characterisation of λ_z .

7.1 Monte Carlo simulation

The level of robustness of each solution produced by the MISOCP model in (57), is calculated as follows:

- (i) Set $n \leftarrow 0$ and $x \leftarrow 0$. Save the binary variables $z_{act,z,k}^*$ and $\omega_{z,k}^*$ generated by the solution of (57).
- (ii) Based on (5)–(6), randomly generate a new set of annual failure rates for every zone as $\lambda_{z,n} \leftarrow \text{Poisson}(\lambda_z)$.
- (iii) Using (36) and (37), recalculate the annual failure rate (Λ_k) and annual interruption duration (U_k) of every node, and determine the new average SAIFI_n and SAIDI_n using (22) and (23).
- (iv) Set $n \leftarrow n + 1$. If SAIFI_n > SAIFI or SAIDI_n > SAIDI, then $x \leftarrow x + 1$. Establish the robustness at iteration n by using the following equation

$$\text{Robustness} = \left(1 - \frac{x}{n}\right) 100\% \quad (58)$$

- (v) If convergence to the first decimal is achieved, then stop; otherwise, return to step ii.

Fig. 5 shows the process of convergence of the Monte Carlo simulations applied to every robust solution in Table 2. Each line in Fig. 5 represents the probability of each robust solution to maintain the system's SAIDI and SAIFI below the limits, even if parameters λ_z randomly changes.

As shown in Table 2, there is a tradeoff between improving the reliability robustness and minimising the active power losses.

Therefore, the proposed methodology is an effective and accurate tool that utilities can use to reconfigure the EDS considering uncertainty in the reliability parameters, depending on their quality of service requirements.

7.2 Reliability robustness versus average reliability optimisation

The minimisation of both reliability indices, SAIDI and SAIFI, assuming the average value of λ_z , does not necessarily lead to robust solutions. To demonstrate this, the robust model in (57) is transformed into a non-robust weighted model given by (59). Note that, the robust reliability constraints (50)–(56) have been removed from (59). Both reliability indices are multiplied by a big positive number M in order to enhance their relative weights in the objective function

$$\begin{cases} \min & c^{iss} \sum_{ij \in \Omega_l} R_{ij} I_{ij}^{sqr} + M(\text{SAIDI} + \text{SAIFI}) \\ \text{s.t.} & (7), (9), (11)–(23), (27)–(41) \end{cases} \quad (59)$$

The non-robust MISOCP model in (59) is convex and can be optimally solved by CPLEX [22]. Table 3 contains the solution of (59) for the 136-node system, using $M = 9999$. A large value of M has been chosen with the aim of forcing the model to improve the average reliability indices. The last column indicates the level of robustness using Monte Carlo simulations as indicated in Section 7.1. Note that, the solution in Table 3 has less robustness than the most robust solution obtained with (57) in Table 2. Therefore, reliability robustness is not guaranteed by the direct minimisation of the average reliability indices.

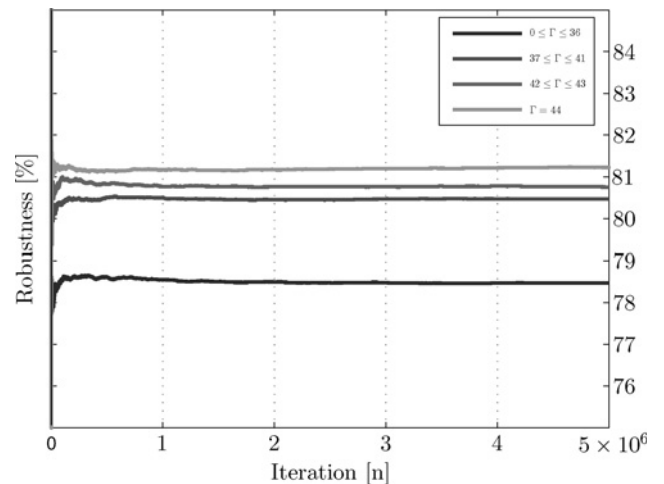
**Fig. 5** Robustness assessment using Monte Carlo simulations

Table 3 Solution of (59) applied to the 136-node system, $M = 9999$

Topology (open switches)	Power losses, kW	SAIDI, [h/cust/yr]	SAIFI, [int/cust/yr]	Robustness, %
12–75, 16–85, 31–136, 39–136, 38–99, 62–99, 62–97, 45–118, 63–108, 8–73, 70–83, 88–103, 42–52, 80–132, 93–94, 24–10	866.7	2.60	2.91	80.4

8 Conclusions

In this paper, a new MISOCP model was proposed to solve the reconfiguration problem of EDS considering the minimisation of active power losses and the robust improvement of the reliability indices, SAIDI and SAIFI. The proposed MISOCP model is a flexible, realistic and precise mathematical approach with convergence to optimality guaranteed by convex optimisation tools.

Uncertainty of the failure rates is a major concern in reliability assessment. As such, this paper presented a robust model that guarantees a reliable operation, even when uncertain reliability parameters change randomly during the real application of the solution. Finally, using Monte Carlo simulations, it has been shown that the model is accurate and that a tradeoff exists between the system topology that improves reliability robustness and the one that minimises active power losses in EDS.

9 References

- IEEE Std. 493-2007: 'IEEE Recommended Practice for the Designing of Reliable Industrial and Commercial Power Systems', 2013
- IEEE Std. 1366-2012: 'IEEE Guide for Electrical Power Distribution Reliability Indices', 2004
- Billinton, R., Allan, R.N.: 'Reliability evaluation of power systems' (Springer, New York, 1996, 2nd edn.), ISBN 978-0306452598
- Merlin, A., Back, H.: 'Search for a minimal-loss operation spanning tree configuration in an urban power distribution system'. Proc. V Power Systems Computer Conf., Cambridge, UK, 1975, pp. 1–18
- Tang, L., Yang, F., Ma, J.: 'A survey on distribution system feeder reconfiguration: Objectives and solutions'. Proc. Innovative 2014 Smart Grid Technologies – Asia, Kuala Lumpur, 2014, pp. 62–67
- Hsiao, Y.-T.: 'Multiobjective evolution programming method for feeder reconfiguration', *IEEE Trans. Power Syst.*, 2004, **19**, (1), pp. 594–599, ISSN 0885-8950
- Mendoza, J.E., Lopez, M.E., Coello, C.A.C., et al.: 'Microgenetic multiobjective reconfiguration algorithm considering power losses and reliability indices for medium voltage distribution network', *IET Gener. Transm. Distrib.*, 2009, **3**, (9), pp. 825–840, ISSN 1751-8687
- Bernardon, D.P., Garcia, V.J., Ferreira, A.S.Q., et al.: 'Multicriteria distribution network reconfiguration considering subtransmission analysis', *IEEE Trans. Power Deliv.*, 2010, **25**, (4), pp. 2684–2691, ISSN 0885-8977
- Amanulla, B., Chakrabarti, S., Singh, S.N.: 'Reconfiguration of power distribution systems considering reliability and power loss', *IEEE Trans. Power Deliv.*, 2012, **27**, (2), pp. 918–926, ISSN 0885-8977
- Vitorino, R., Jorge, H., Neves, L.: 'Loss and reliability optimization for power distribution system operation', *Electr. Power Syst. Res.*, 2013, **96**, pp. 177–184, ISSN 0378-7796
- Kavousi-Fard, A., Akbari-Zadeh, M.-R.: 'Reliability enhancement using optimal distribution feeder reconfiguration', *Neurocomputing*, 2013, **106**, pp. 1–11, ISSN 0925-2312
- Kavousi-Fard, A., Niknam, T.: 'Multi-objective stochastic distribution feeder reconfiguration from the reliability point of view', *Energy*, 2014, **64**, (0), pp. 342–354, ISSN 0360-5442
- Kavousi-Fard, A., Niknam, T.: 'Optimal distribution feeder reconfiguration for reliability improvement considering uncertainty', *IEEE Trans. Power Deliv.*, 2014, **29**, (3), pp. 1344–1352, ISSN 0885-8977
- Esmailian, H.R., Fadaeimedjad, R., Attari, S.M.: 'Distribution network reconfiguration to reduce losses and enhance reliability using binary gravitational search algorithm'. Proc. of the 22nd Int. Conf. and Exhibition on Electricity Distribution, Stockholm, 2013, pp. 1–4
- Alonso, F., Oliveira, D., Zamboni de Souza, A.: 'Artificial immune systems optimization approach for multiobjective distribution system reconfiguration', *IEEE Trans. Power Syst.*, 2015, **30**, (2), pp. 840–847, ISSN 0885-8950
- Gupta, N., Swarnkar, A., Niazi, K.: 'Distribution network reconfiguration for power quality and reliability improvement using genetic algorithms', *Int. J. Electric. Power Energy Syst.*, 2014, **54**, (0), pp. 664–671, ISSN 0142-0615
- Narimani, M.R., Vahed, A.A., Azizpanah, R., et al.: 'Enhanced gravitational search algorithm for multi-objective distribution feeder reconfiguration

- considering reliability, loss and operational cost', *IET Gener. Transm. Distrib.*, 2014, **8**, (1), pp. 55–69, ISSN 1751-8687
- Carcamo-Gallardo, A., Garcia-Santander, L., Pezoa, J.: 'Greedy reconfiguration algorithms for medium-voltage distribution networks', *IEEE Trans. Power Deliv.*, 2009, **24**, (1), pp. 328–337, ISSN 0885-8977
- Duan, D.-L., Ling, X.-D., Wu, X.-Y., et al.: 'Reconfiguration of distribution network for loss reduction and reliability improvement based on an enhanced genetic algorithm', *Int. J. Electric. Power Energy Syst.*, 2015, **64**, (0), pp. 88–95, ISSN 0142-0615
- Bertsimas, D., Sim, M.: 'The price of robustness', *Oper. Res.*, 2004, **52**, (1), pp. 35–53, ISSN 0030-364X
- Fourer, R., Gay, D.M., Kernighan, B.W.: 'AMPL: a modeling language for mathematical programming' (Brooks/Cole-Thomson Learning, Pacific Grove, CA, 2003, 2nd edn.), ISBN 978-0534388096
- CPLEX Optimization Subroutine Library Guide and Reference, ILOG Inc., Incline Village, NV, CPLEX division edn., 2008
- Céspedes, R.: 'New method for the analysis of distribution networks', *IEEE Trans. Power Deliv.*, 1990, **5**, (1), pp. 391–396, ISSN 0885-8977
- Shimohammadi, D., Hong, H.W., Semlyen, A., et al.: 'A compensation-based power flow method for weakly meshed distribution and transmission networks', *IEEE Trans. Power Syst.*, 1988, **3**, (2), pp. 753–762, ISSN 0885-8950
- Lavorato, M., Franco, J.F., Rider, M.J., et al.: 'Imposing radiality constraints in distribution system optimization problems', *IEEE Trans. Power Syst.*, 2012, **27**, (1), pp. 172–180, ISSN 0885-8950
- Romero-Ramos, E., Riquelme-Santos, J.: 'Discussion on 'imposing radiality constraints in distribution system optimization problems'', *IEEE Trans. Power Syst.*, 2013, **28**, (1), pp. 568–568, ISSN 0885-8950
- Romero-Ramos, E., Riquelme-Santos, J., Reyes, J.: 'A simpler and exact mathematical model for the computation of the minimal power losses tree', *Electr. Power Syst. Res.*, 2010, **80**, (5), pp. 562–571, ISSN 0378-7796
- Borges, M.C.O., Franco, J.F., Rider, M.J.: 'Optimal reconfiguration of electrical distribution systems using mathematical programming', *J. Control Autom. Electr. Syst.*, 2014, **25**, (1), pp. 103–111
- Franco, J.F., Rider, M.J., Romero, R.: 'A mixed-integer quadratically-constrained programming model for the distribution system expansion planning', *Int. J. Electric. Power Energy Syst.*, 2014, **62**, pp. 265–272, ISSN 0142-0615
- Bazaraa, M.S., Jarvis, J.J., Sherali, H.D.: 'Linear programming and network flows' (John Wiley & Sons, New York, 2009, 4th edn.), ISBN 978-0470462720
- 136 Buses, 156 Branches Medium City Real Distribution System for Network Reconfiguration, URL <http://www.feis.unesp.br/#!/departamentos/engenharia-eletrica/pesquisas-eprojeto/lapsee/downloads/>, 2015
- Procedimentos de Distribuição de Energia Elétrica no Sistema Elétrico Nacional – PRODIST. Módulo 8 – Qualidade da Energia Elétrica, Agência Nacional de Energia Elétrica, Brasília, DF, 2012

10 Appendix

The linear robust programming approach proposed by Bertsimas and Sim [20] is able to maintain model feasibility even if the uncertain parameters stochastically change without excessively deteriorate the objective function.

Consider the linear optimisation problem given by the following equation

$$\begin{cases} \min \sum_j c_j x_j \\ \text{s.t.} \\ \sum_j a_{ij} x_j \leq b_i \quad \forall i \\ l_j \leq x_j \leq u_j \quad \forall j \end{cases} \quad (60)$$

where x_j is the set of decision variables, c_j is the set of costs at the objective function and a_{ij} is the set of coefficients for every constraint i and variable j . Consider that Ω_{U_i} contains all of the coefficients in the i th constraint that are subject to uncertainty, and every uncertain parameter a_{ij} , $\forall j \in \Omega_{U_i}$ is modelled as a random variable that takes values within the symmetric and bounded interval $[a_{ij} - \hat{\alpha}_{ij}, a_{ij} + \hat{\alpha}_{ij}]$, where a_{ij} represents the mean value, and $\hat{\alpha}_{ij}$ represents the maximum positive deviations around the mean value.

A new parameter Γ_i for every constraint i is introduced. Γ_i controls the number of uncertain variables that can stochastically change without violating the i th constraint. Thus, Γ_i can only take values between 0 and $|\Omega_{U_i}|$. With this in mind, the non-linear formulation in (60) is the mathematical model that makes possible to adjust the

level of robustness of the final solution depending on the value of Γ_i .

$$\begin{cases} \min \sum_j c_j x_j \\ \text{s.t.} \\ \sum_j a_{ij} x_j + \max_{S_i | S_i \subseteq \Omega_{U_i}, |S_i| = \Gamma_i} \left\{ \sum_{j \in S_i} \hat{a}_{ij} |x_j| \right\} \leq b_i \quad \forall i \\ l_j \leq x_j \leq u_j \quad \forall j \end{cases} \quad (61)$$

To linearise the formulation in (61), the term

$$\beta_i(\mathbf{x}, \Gamma_i) = \max_{S_i | S_i \subseteq \Omega_{U_i}, |S_i| = \Gamma_i} \left\{ \sum_{j \in S_i} \hat{a}_{ij} |x_j| \right\}$$

is evaluated in a given solution \mathbf{x}^* and transformed into a linear programming problem given by the following equation

$$\begin{cases} \beta_i(\mathbf{x}^*, \Gamma_i) = \max \sum_{j \in \Omega_{U_i}} \hat{a}_{ij} |x_j^*| z_{ij} \\ \text{s.t.} \\ \sum_{j \in \Omega_{U_i}} z_{ij} \leq \Gamma_i \\ 0 \leq z_{ij} \leq 1 \quad \forall j \in \Omega_{U_i} \end{cases} \quad (62)$$

Clearly, the solution of (62) determines the maximum possible deviation of the constraint i , if Γ_i parameters are allowed to

change. The dual model of (62) is given by (63) for every constraint i .

$$\begin{cases} \min \sum_{j \in \Omega_{U_i}} p_{ij} + \Gamma_i z_i \\ \text{s.t.} \\ z_i + p_{ij} \geq \hat{a}_{ij} |x_j^*| \quad \forall i, \forall j \in \Omega_{U_i} \\ p_{ij} \geq 0 \quad \forall j \in \Omega_{U_i} \\ z_i \geq 0 \quad \forall i \end{cases} \quad (63)$$

Replacing the term $\beta_i(\mathbf{x}, \Gamma_i)$ in (60) by the objective function of (63), and adding the new set of dual constraints, the non-linear robust formulation in (61) is transformed into the equivalent linear formulation shown in the following equation

$$\begin{cases} \min \sum_j c_j x_j \\ \text{s.t.} \\ \sum_j a_{ij} x_j + z_i \Gamma_i + \sum_{j \in \Omega_{U_i}} p_{ij} \leq b_i \quad \forall i \\ z_i + p_{ij} \geq \hat{a}_{ij} |x_j| \quad \forall i, \forall j \in \Omega_{U_i} \\ l_j \leq x_j \leq u_j \quad \forall j \\ p_{ij} \geq 0 \quad \forall i, \forall j \in \Omega_{U_i} \\ z_i \geq 0 \quad \forall i \end{cases} \quad (64)$$

The formulation in (64) is a linear adjustable robust approach used to protect the original model from being unfeasible even when the uncertain parameters randomly change.